Laser synthesis of nanomaterials for nuclear nanomedicine

Gleb Tikhonowski, Anton Popov, Ivan Zelepukin, Elena Popova-Kuznetsova, Yaroslava Dombrovska, Sergey Deev, Irina Zavestovskaya, Sergey Klimentov, Paras Prasad, Andrei Kabashin

Laser-ablative synthesis of nanomaterials for nuclear and radiative medicine applications

G. V. Tikhonowski[a*], A. A. Popov[a], I. Zelepukin[a,b], E. Popova-Kuznetsova[a], Y. Dombrovska[a], S. M. Deyev[a,b], I. N. Zavestovskaya[a,c], S. M. Klimentov[a], P. N. Prasad[a,d] and A.V. Kabashin[a,e*]

[a] MEPHI, Institute of Engineering Physics for Biomedicine, Kashirskoe sh. 31, 115409 Moscow, Russia; [b] Shemyakin-Ovchinnikov Institute of Bioorganic Chemistry, Miklukho-Maklaya st. 16/10, 117997, Moscow, Russia; [c] P. N. Lebedev Physical Institute of the RAS, Leninsky avenue 53, 119991, Moscow, Russia; [d] Department of Chemistry and Institute for Lasers, Photonics, and Biophotonics, University at Buffalo, The State University of New York, Buffalo, NY 14260, USA; [e] Aix Marseille Univ., CNRS, LP3, Campus de Luminy, Case 917, 13288 Marseille, France;

*E-mail: gvtikhonovskii@mephi.ru, andrei.kabashin@univ-amu.fr

ABSTRACT

Newly emerging nanomaterials promise a major advancement of methods of nuclear and radiative medicine for cancer treatment, as they can be used as carriers of diagnostic or therapeutic radionuclides, contrast agents in nuclear imaging modalities (PET, SPECT) or sensitizers of radiative therapies (X-ray, ion beams, etc.). However, nanotechnology-based approaches have reported a limited success so far due to a lack of suitable functional nanoformulations, which are safe, non-toxic, excretable from the body and have favorable pharmacokinetics for effective accumulation in the tumor. As follows from the results of our on-going research activities, many of the above-stated problems can we solved by the employment of nanomaterials fabricated by clean laser-ablative synthesis. Here, we review our recent data on some promising nanomaterials, prepared by this method, including biodegradable silicon (Si) nanoparticles (NPs), ^{152}Sm-enriched samarium oxide NPs, and elemental bismuth (Bi) NPs, which can be used either as carriers/agents in radionuclide therapy, or sensitizers in radiative diagnostics or therapy. Advantages of proposed approach include exceptional purity and flexibility in synthesizing of NPs of required physico-chemical parameters (controlled size, shape, composition, and surface conditioning of NPs). Advances in laser-ablative fabrication of novel nanomaterials open up avenues for future implementations of nuclear and radiative medicine approaches for safe and efficient theranostics of tumors and metastasis.

Keywords: Nanoparticles, pulsed laser ablation in liquids, nuclear medicine, radiative medicine, carriers of radionuclides, silicon nanoparticles, samarium nanoparticles, bismuth nanoparticles.

1. INTRODUCTION

Methods of nuclear and radiative medicine have become increasingly popular for last decades, promising an efficient powerful alternative to conventional chemotherapy[1]. The nuclear medicine modality implies an injection of short decay time radionuclides in vivo (systemically or intratumorally), while their ionizing radiation (α, β, γ) is used to damage the DNAs of actively proliferating cancer cells, thus causing their selective death, while keeping normal cells weakly affected[1]. The radionuclide therapy becomes especially efficient when one can achieve a high tumor/non-tumor radionuclide contrast, which enables to minimize side effects related to the irradiation of healthy issues. Typically, vectoring molecules (specific antibodies, etc.) are used to target radionuclides to the tumor, but these molecules are typically small and can carry only a few chelates linked to radionuclide atoms[2]. Therefore, very high concentrations of radionuclide-carrying molecules are required to achieve any therapeutic outcome, but this can lead to severe side effects. The employment of nanomaterials as carriers of radionuclides promises a solution of radionuclide delivery problem, as they are heavier and can have much higher loading capacity[3,4], as well as can offer an additional passive mechanism for targeting tumors based on the enhanced permeability and retention (EPR) effect[5]. Despite these promises, this field has seen limited activities, primarily because of a lack of suitable nanocarriers, which are safe, excretable and have favorable

pharmacokinetics to efficiently deliver and retain radionuclides in a tumor. On the other hand, radiative nanomedicine is based on the employment of radioactive beams (X-ray, neutron, proton, and ion) to diagnose and treat tumors[6-8]. To improve the treatment outcome, NPs of high-Z elements can be used as a sensitizer of therapeutic (photon-capture therapy, γ-therapy) and diagnostic (CT imaging) impacts[9,10]. When these high-Z elements are irradiated with X-rays, the result is a high local ionization effect leading to DNA strand breaks and ultimately enhancing the efficacy of RT. Off target damage is also limited, as the range of this effect is less than 10 nm; consequently, lower doses of RT can be used to achieve the desired effects[10].

However, the synthesis of nanoformulations for nuclear and radiative medicines presents a major challenge due to a series of stringent requirements, including the following: (i) NPs should have appropriate physico-chemical parameters (size, shape, chemical composition, surface properties, etc.) to provide efficient radionuclide transport properties, or enable imaging/therapy functionalities under radiative stimuli; (ii) they should be safe and excretable from the organism to minimize toxicity and residual accumulation risks; (iii) they should have a targeting ability to effectively localize in high concentrations in the tumor. Unfortunately, these requirements are difficult or impossible to meet using conventional chemical or alternative methods. As an example, chemical synthesis pathways typically deal with fixed chemical products under fixed ambient conditions, which complicates the achievement of particular physico-chemical properties of nanomaterials, as well as leads to the contamination of formed nanoformulations by reaction by-products (toxic in most cases). Alternative synthesis pathways are also not free of challenges and limitations to fabricate chemically pure nanomaterials with desired physico-chemical characteristics and good dispersion in aqueous environment.

Pulsed laser ablation in liquids presents a physical alternative, which can offer the flexibility in the synthesis of single or multi-elemental nanoformulations in the absence of residual contamination by by-products of synthesis[11,12]. This approach relies on laser radiation-caused ablation of material from a solid target to initiate the generation of nanoclusters[13], which can then be released either into a gaseous medium to form a substrate-supported nanostructured film or a powder[14-17], or into a liquid medium to form a dispersion of NPs[18-24]. In all cases, the ablation can be performed in an ultrapure environment (inert gas, deionized water, etc.) to exclude any contamination of the nanoparticle surface by side-products or stabilizing ligands, which is critically important for projected biomedical applications in vitro and in vivo[25,26]. As an example, we recently elaborated the technique of femtosecond (fs) laser ablation in water and organic media, which renders possible an efficient control of size characteristics of NPs from a variety of materials, including Au[22,27,28], Ag[23], Si[29,30], TiN[31-33] NPs, which demonstrate unique characteristics for biomedical tasks.

As follows from the results of our on-going activities, laser-ablative synthesis provides unique opportunities for the fabrication of nanomaterials for nuclear and radiative medicine. As an example, owing to excellent fast biodegradability, laser-ablated Si NPs functionalized with PEG can act as a nearly ideal carrier of radionuclides for nuclear nanomedicine[34]. We recently demonstrated such an opportunity by a coating of laser-synthesized Si NPs by PEG and a fast conjugation of the Si NPs-PEG complex with the ^{188}Re radionuclide, which is one of most promising generator-type therapeutic β-emitters with the energy of positron emission of 1.96 MeV (16.7%) and 2.18 MeV (80%) and the half-decay time of 17 hours[1]. We showed that such Si NPs-PEG-^{188}Re conjugates can efficiently deliver the radionuclide through the blood stream and retain it in the tumor region, yielding an excellent therapeutic effect (72% survival compared to 0% of the control group). On the other hand, the flexibility of laser-ablative synthesis makes possible the fabrication of novel promising nanomaterials for nuclear and radiative medicine. In particular, we described the synthesis of stable solutions of spherical and size-tunable (7–70 nm) ^{152}Sm-enriched samarium oxide NPs[35], which can be suitable for nuclear nanomedicine tasks after activation in a nuclear reactor and appropriate biofunctionalization to minimize immune response and target tumors. Finally, we demonstrated the possibility of synthesizing elemental bismuth (Bi) NPs via fs-laser ablation in water and organic solvents and described a protocol for the preparation of stable aqueous solutions of Bi NPs covered with Pluronic®F68 and Pluronic® F127[36]. The formed Bi NPs promise attractive applications in radiative medicine, as bismuth has the highest atomic number of all non-radioactive elements leading to excellent radiosensitization properties[9].

In this short review article, we will summarize our recent progress in the laser-ablative fabrication and characterization of nanomaterials for nuclear and radiative medicine (Si NPs, ^{152}Sm-enriched samarium oxide NPs, Bi NPs) and review first results on the application of these nanomaterials in these tasks.

2. EXPERIMENTAL METHODOLOGY FOR LASER-ABLATIVE SYNTHESIS

Nanoformulations for nuclear and radiation nanomedicine were synthesized by fs pulsed laser ablation. A schematic of the experimental setup is shown in Figure 1. Briefly, the target was fixed vertically with a PTFE stand in a glass (BK-7) vessel filled with a liquid. A 3-mm-diameter beam from a Yb:KGW laser (1030 nm wavelength, 270 fs pulse duration, 30 μJ pulse energy, 100 kHz repetition rate; TETA 10 model, Avesta, Moscow, Russia) was focused by a 100-mm F-theta lens on the surface of different targets, through a side wall of the ablation vessel. The thickness of the liquid layer along the laser beam was 3-6 mm. The focusing conditions were set to obtain maximum productivity from the ablation process (defined as ablated mass per duration of ablation) individually for each material. The laser beam was moved over a 20 × 20 mm area with self-closed spiral geometry on the surface of the target, with 4000 mm/s speed using a galvanometric scanner. This was done to avoid drilling of a hole in the target and to maximize the NPs yield. The duration of each laser ablation experiment was 30 min. The target and the ablation chamber were cleaned after each ablation experiment, by using an ultrasonication step in acetone, followed by ultrasonication in water, thorough rinsing in ultrapure water and, finally, drying under ambient conditions.

In some cases, we used a technique of femtosecond laser fragmentation from nano/microcolloids, which were formed prior to the fragmentation experiments by laser ablation from a target (according to the description given above) or a mechanical milling of wafer (in the case of silicon). Nano/microcolloids were water-dispersed and then fragmented under laser irradiation for one hour. The laser beam was focused at 1cm below the water level, while the solution was continually homogenized by a magnetic stirrer as shown under the label (5) in the Figure 1.

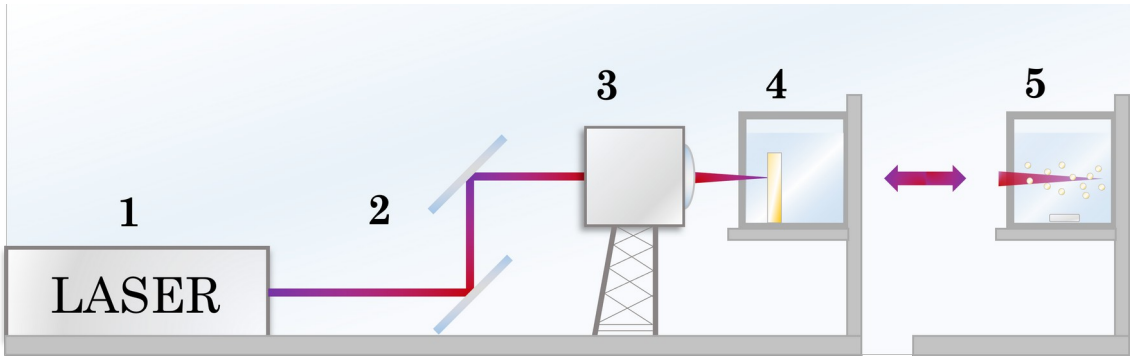

Figure 1. Schematic representation of experimental setup: (1) – fs laser, (2) – dielectric mirrors, (3) – galvanometric scanner, (4) – filled with liquid ablation vessel with a target, (5) – fragmentation vessel with a NPs colloidal solution and a magnet stirrer.

To determine the size and morphology characteristics of NPs, a high-resolution transmission electron microscopy (HR-TEM) system (JEOL JEM 3010) and a scanning electron microscope (SEM) system (TESCAN MAIA 3) operating at 0.1 – 30 kV were used. A 1μL droplet of solution containing laser-synthesized NPs was deposited onto the surface of a carbon-coated TEM copper grid or a cleaned silicon substrate (SEM imaging) and dried under ambient conditions. DLS size distributions and ζ–potential measurements were performed using a Zetasizer ZS instrument (Malvern Instruments, Orsay, Paris, France).

3. RESULTS AND DISCUSSION

3.1 Laser-ablative fabrication of Si NPs-PEG-^{188}Re conjugates in mice, assessment of their biodistribution and therapeutic outcome

The uniqueness of such Si NPs is related to their high biocompatibility and biodegradability, which makes possible elimination of these structures from the organism within several days, even if their initial size is large (30–80nm)[29,30], under absence of any toxic effects. In addition, in contrast to Si nanostructures prepared by conventional electrochemical or chemical routes[37], laser-synthesized Si NPs have ideal for biomedical implementation spherical morphology,

controllable size with a narrow size dispersion, and are free of any toxic impurities[30], which promises a better transport in vivo and no side effects.

In our experiments, NPs were fabricated by methods of laser ablation from a solid Si target (N-type, purity 99.999%) or laser fragmentation[34]. The functionalization of Si NPs with PEG was performed as shown in Figure 2. The Si NPs were dispersed in 10 mL of 96% ethanol to a final concentration of 2g/L. Then, 200 mg of the silane-PEG-COOH solution in 20 mL of ethanol was added to the NPs under continuous stirring at room temperature. Since only dense coating of the NPs by PEG can provide stealth properties, we used a large molar excess of the silane-PEG chains in this reaction. The resulting mixture was ultra-sonicated for 1 min, and 1 mL of 3% ammonium hydroxide was quickly drop added into the mixture under vigorous stirring to catalyze the hydrolysis and condensation of the silane groups on the surface of the Si NPs. Then we tested if the pH of the mixture had reached 9–10 and heated this solution for 2.5h at 70°C. To prevent further hydrolysis and self-aggregation of unreacted silanes, the mixture was cooled down to the room temperature and the NPs were washed by centrifugation (15 min, 5000g), firstly with pure ethanol and further with water 3 times. After washing, the product was redispersed in 20 mL of PBS (pH 7.4). The obtained NPs suspension did not contain any aggregates and had long-term colloidal stability at physiological conditions, as was confirmed by Dynamic Light Scattering (Zetasizer Nano ZS, Malvern Instruments, UK). Also, we observed a strong negative zeta-potential after coupling of the PEG-COOH chains with the silicon surface. All the measurements were conducted in MilliQ water.

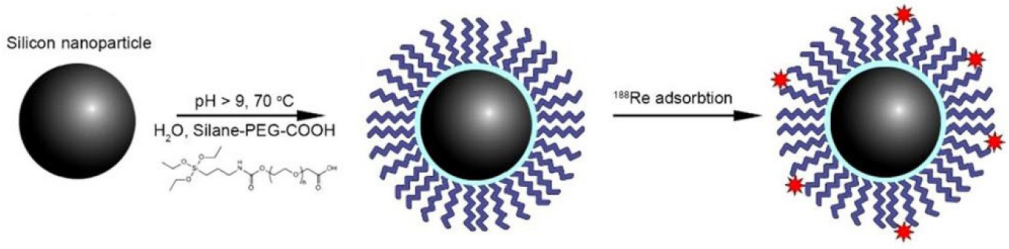

Figure 2. Schematic presentation of functionalization protocol for the coating of Si*NPs by polyethylene glycol (PEG) and subsequent decoration by radioactive ^{188}Re atoms. Adapted from F[34].

In our tests, biodistribution of the nanoparticle carrier-based Si NPs-PEG-^{188}Re conjugate was compared with that of freely circulating radioactive rhenium using its salt sodium perrhenate form, Na^{188}ReO$_4$. Five sub-groups of 4 Wistar female rats from the "signal" group, implanted with liver cholangioma RS-1, were intravenously administered with a single dose of 56.8–62.5μg/kg of animal weight of Si NPs-PEG-^{188}Re conjugates. Similar number of animals from the "control" group were injected with water dissolved Na^{188}ReO$_4$, containing radioactive rhenium atoms at the same concentration. The maximal level of radioactivity in blood was recorded after 5 minutes of injection of both Si NPs-PEG-^{188}Re and Na^{188}ReO$_4$ solutions which then gradually decreased. For free ^{188}Re (in ^{188}ReO$_4^-$), the level of radioactivity in blood was much lower (<0.5%, after 5min; <0.2% after 1hour, <0.1% after 24 hours, and finally not detectable after 48 hours). At the same time, the injection of free Na^{188}ReO$_4$ was accompanied by an immediate increase of the ^{188}Re concentration mainly in the thyroid gland, reaching its maximum values of 17% 3hours after the radionuclide injection. The accumulation of ^{188}Re in other organs was much lower, although we recorded a certain concentration of ^{188}Re in the stomach just after the injection (1.2% after one hour), and its smaller concentrations in lungs and kidneys (less than 0.25% and 0.3%, respectively, after five minutes). Notice that the recorded biodistribution and pharmcokinetics with much preferable accumulation of the product in thyroid gland and stomach is typical for free ^{188}Re and other radionuclides[1].

Surprisingly, the accumulation of radionuclide in liver and spleen was very weak (less than 2.5% and 0.3% after 5 minutes and then rapidly decreased down to 0.5–0.7% and 0.05% after 24 hours, respectively). The absence of any significant accumulation of Si NPs-PEG-^{188}Re conjugates in organs of reticuloendothelial system (liver, spleen) can only be explained by their invisibility to the immune system, which was obviously due to the PEG-based coating of Si NPs. Such a coating led to prolonged circulation of Si NPs-PEG-^{188}Re conjugates in the blood stream and their efficient delivery to most organs. It is also important that the concentration of ^{188}Re gradually increased in the kidneys, reaching its maximal value 24 hours after the injection (almost 3%), which is consistent with gradual dissolution of nanoformulations and their time-delayed elimination via renal clearance. For comparison, in the case of free rhenium

(injection of $Na^{188}ReO_4$ solutions) its concentration in the kidney was maximal just after the injection (5 min), which can lead to undesirable kidneys damage.

The therapeutic efficiency of Si NPs-^{188}Re conjugates was assessed by using Wistar rats with cholangioma RS-1 implanted in the right femoral muscle. We used 30 rats divided into three sub-groups of 10 animals: the 1st and 2nd "signal" groups were intratumorally administered with a single dose of 37 and 74 MBq of NPs carrier-based Si NPs-PEG-^{188}Re conjugates, respectively, while the 3rd "control" group were intratumorally injected by 0.1mL of physiological solutions. Figure 3 shows results of survival tests for these 3 groups. One can see that after 20 days, only 40% of rats from the control group survived, while the survival rate for the 1st and 2nd "signal" groups was 100%. After 30 days, all animals from the control group were dead, while the survival rate for the 1st and 2nd groups was 50% and 72%, respectively. Thus, our experiments clearly demonstrate a remarkable therapeutic effect under intratumoral injection of the Si NPs-PEG-^{188}Re conjugates. It should be noted that the accomplished injection protocol was not optimized to maximize the therapeutic effect. We believe that the efficiency of the treatment can still be improved, e.g., by using 2 and more injections and further optimization of dose radioactivity.

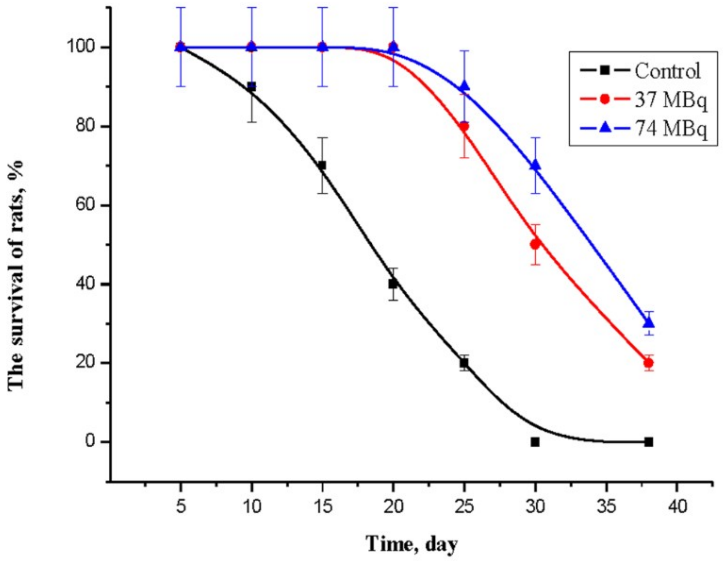

Figure 3. Assessment of therapeutic effect. Survival curves for Wistar rats with implanted cholangioma RS-1 after intratumoral injection of the Si NPs-PEG-^{188}Re conjugates providing different doses of radioactivity (37 and 74 MBq) and for control group injected with physiological solutions. Each group was composed of 10 animals. Adapted from [34].

We believe that the demonstrated ability of Si NPs to serve as efficient transport vehicle can be used with a variety of other promising diagnostic and therapeutic radionuclides (e.g., ^{64}Cu, ^{68}Ga, ^{90}Y). It is also important that intrinsic properties of laser-synthesized Si NPs make possible a series of unique imaging and therapy functionalities, including photoluminescence[38] and non-linear optical[39] responses for bioimaging, light-induced generation of singlet oxygen for photodynamic therapy of cancer[40], infrared radiation-induced[41] or radio frequency radiation-induced[42] hyperthermia-based cancer therapy. In fact, the choice of Si NPs as radionuclide carrier means that all these imaging and therapy modalities can be utilized in parallel with the main nuclear medicine modality to produce image guided therapy.

3.2 Laser-ablative synthesis and characterization of ^{152}Sm-enriched samarium oxide NPs

^{152}Sm isotope enriched Sm oxide NPs are another promising functional nano-radiopharmaceutical for nuclear nanomedicine. This isotope captures neutrons by a nuclear reaction to produce the short-lived samarium-based radio isotope ^{153}Sm, which is known as one of most promising β-emitters for the treatment of malignant tumors, including lung, prostate, and breast cancers[43,44]. Nanoformulations of ^{152}Sm-enriched samarium compounds are of great value for advancing nuclear nanomedicine as it can provide a high local concentration of the radioisotope, which cause dramatical reduce of the effect of radiation dose on healthy tissues.

Colloidal solutions of bare Sm oxide NPs were prepared by two-step fs laser ablation (first step - laser ablation, second - laser fragmentation) of a bulk Sm oxide target in water, as described in detail in[35]. For preparation of Sm oxide target, we used Sm_2O_3 micropowder enriched with ^{152}Sm isotope (97.78–98.70%, purity 99.80%) purchased from Elektrokhimpribor Combine (Lesnoy, Russia). The average grain size of the initial micro powder was 0.5–2 μm. The target was prepared as follows: five milligrams of the powder was pressed into a cylindrical pellet having 5 mm diameter and 150 μm thickness. The pellet was then glued to a silicon substrate using epoxy glue to form the ablation target. Since the glue was used only on the back side of the pellet in order to fix it on the silicon substrate, it was not affected by laser radiation during our experiments. The target preparation process is shown schematically in Figure 4.

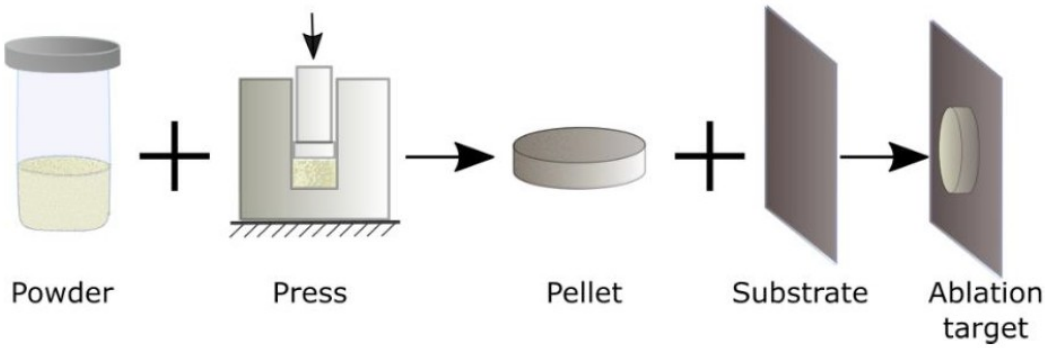

Figure 4. Schematic representation of ablation target preparation. The initial Sm_2O_3 micro powder was pressed into a cylindrical pellet, which was then glued to a silicon wafer to form the ablation target. Adapted from [35].

The ablation was performed with different pulse energies ranging from 10 up to 100 μJ, which resulted in NPs solutions of 30–50 μg/mL concentrations. In all cases, the obtained solutions were almost completely transparent, with a slight whitish coloration. Typical TEM images of Sm oxide NPs synthesized by the ablation from the target under 50 μJ pulse energy is shown in Figure 5a. One can see that the formed NPs had a broad dispersion, which could be approximated by 2 Gaussian functions with maxima at 30 and 70 nm. The composition of synthesized NPs was qualitatively analyzed by energy-dispersive X-ray spectroscopy (EDS). A typical EDS spectrum is shown in Figure 5c. As one can see from the figure, NPs were mainly composed of samarium and oxygen.

One-step laser ablation cannot provide good control of size characteristics, as formed NPs have a large mean size and are size- and shape-dispersed. Such characteristics are hardly consistent with projected applications. To homogenize size distributions, we applied the technique of femtosecond laser fragmentation in liquids (LFL), which was developed in our earlier works to reduce the size of Au NPs[27]. The technique implies irradiation of a preliminary prepared colloidal solution by a focused fs laser beam. This approach profits from a significant broadening of an intense fs laser spectrum and a generation of a so-called white light supercontinuum, which leads to efficient fragmentation of almost any NPs, regardless of their absorption profile. The results of such an additional laser treatment are shown in Figure 5 (c) and (d) respectively. As one can see, the fs LFL not only allows one to drastically decrease the size of NPs and narrow down their size distribution, but also provides a size control. Indeed, a prolonged LFL with 50 μJ pulse energy led to a log-normal size distribution of Sm oxide NPs with 20 nm mean diameter and 10 nm FWHM width, while LFL with 100 μJ pulse energy resulted in NPs with 7 nm mean diameter.

After the fragmentation process, we found that the remaining solutions were stable and did not show any traces of precipitation during their storage under room conditions for several months. Such a good colloidal stability of bare laser-synthesized colloids is dictated by electrical charging of NPs during the ablation process and related electrostatic stabilization. Indeed, according to our ζ—potential measurements, the surface potential of the laser-ablated Sm oxide NPs was +20 mV which coincides with the stability threshold for colloidal solutions.

The final product presented NPs with a narrow size dispersion and variable mean size. ^{152}Sm-enriched samarium oxide NPs can be used an efficient β-emitter for nuclear nanomedicine tasks after activation in a nuclear reactor and appropriate biofunctionalization to minimize immune response and target tumors. The formed NPs with bare, ligand-free

surface and high colloidal stability are of great interest as a novel and perspective nanoplatform for biomedical and catalysis applications.

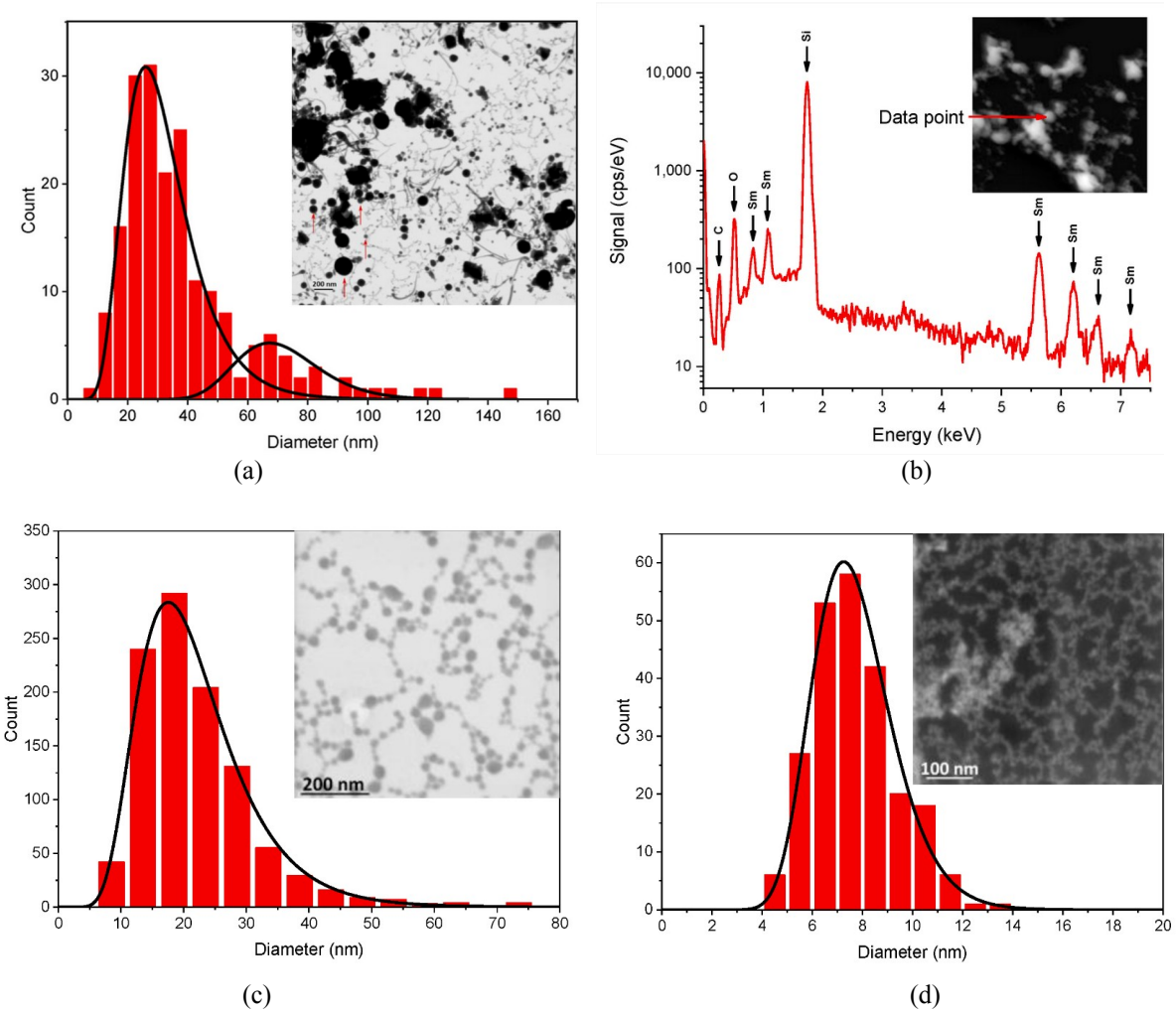

Figure 5. Typical TEM image and size distribution of Sm oxide NPs (a) obtained by laser ablation with 50 µJ and their EDS spectrum (b). The silicon peak is related to the Si substrate, while the carbon signal is related to organic contamination of the vacuum chamber. Size distributions with typical scanning transmission electron microscopy (STEM) images of Sm oxide NPs after fs laser fragmentation in water under pulse energies of 50 µJ (c) and 100 µJ (d). Adapted from [35].

3.3 Laser-ablative synthesis and characterization of bare elemental Bi NPs

Presenting a semimetal/metal having the highest atomic number among all non-radioactive elements, elemental bismuth (Bi) nanoparticles (NPs) with the highest number density of Bi nuclei, could serve as efficient targeted agents for cancer treatment, including contrast agents for CT imaging, sensitizers for image guided X-Ray radiotherapy and photothermal therapy[9,10]. However, the synthesis of elemental Bi NPs to achieve the highest Bi atom concentration suitable for biological applications is difficult using conventional chemical routes. In our study, we explored the fabrication of ultrapure Bi-based nanomaterials by fs laser ablation from a solid Bi target in liquid ambient (deionized water and acetone) and characterized them techniques[36].

Laser ablation of the Bi target in acetone (LAA) and deionized water (LAW) resulted initially in dark-brown colloidal solutions. During the first 5–10 min of the ablation process, there was no visible difference in color of solutions being

prepared in any solvents; however, by the end of an ablation experiment (15 min), water-based colloidal solution became substantially turbid, while those prepared in acetone remained clear. NPs prepared by LAW further changed their color to milky-white after approximately 100 min. STEM images taken several days after the preparation revealed significant differences in sizes and morphologies of Bi-based nanomaterials synthesized by LAA and LAW (Figure 6a and 6b). As a result, we found that LAA leads to the formation of strictly spherical Bi NPs with bimodal size distribution. The distribution peaks are at 20–30 nm and 60-70 nm. At the same time, LAW leads to the formation of 400–500 nm flake-like nanosheets wide size dispersion, sharp edges, and a thickness of 10–20 nm. An X-ray diffraction (XRD) pattern of the Bi NPs generated by fs LAA is shown in Figure 6c. All the peaks can be indexed with the reference data for Bi metal (ICDD, No. 00-44-1246) with lattice parameters, a = 4.547 Å and c =11.862 Å; no impurity phase is present, indicating LAA generates pure Bi metal NPs. The XRD pattern of the nanosheets generated by Bi fs LAW can be seen in Figure 6d. Most of the diffraction lines are indexed with the reference data for $(BiO)_2CO_3$ (ICDD No. 00-025-1464). Some peaks characteristics of $(BiO)_4CO_3(OH)_2$ (ICDD 00-038-0579) were also observed at 11.99, 29.45, 36.50, and 50.19°. This suggests that Bi LAW results in nanosheets containing a combination of both $(BiO)_2CO_3$ and $(BiO)_4CO_3(OH)_2$.

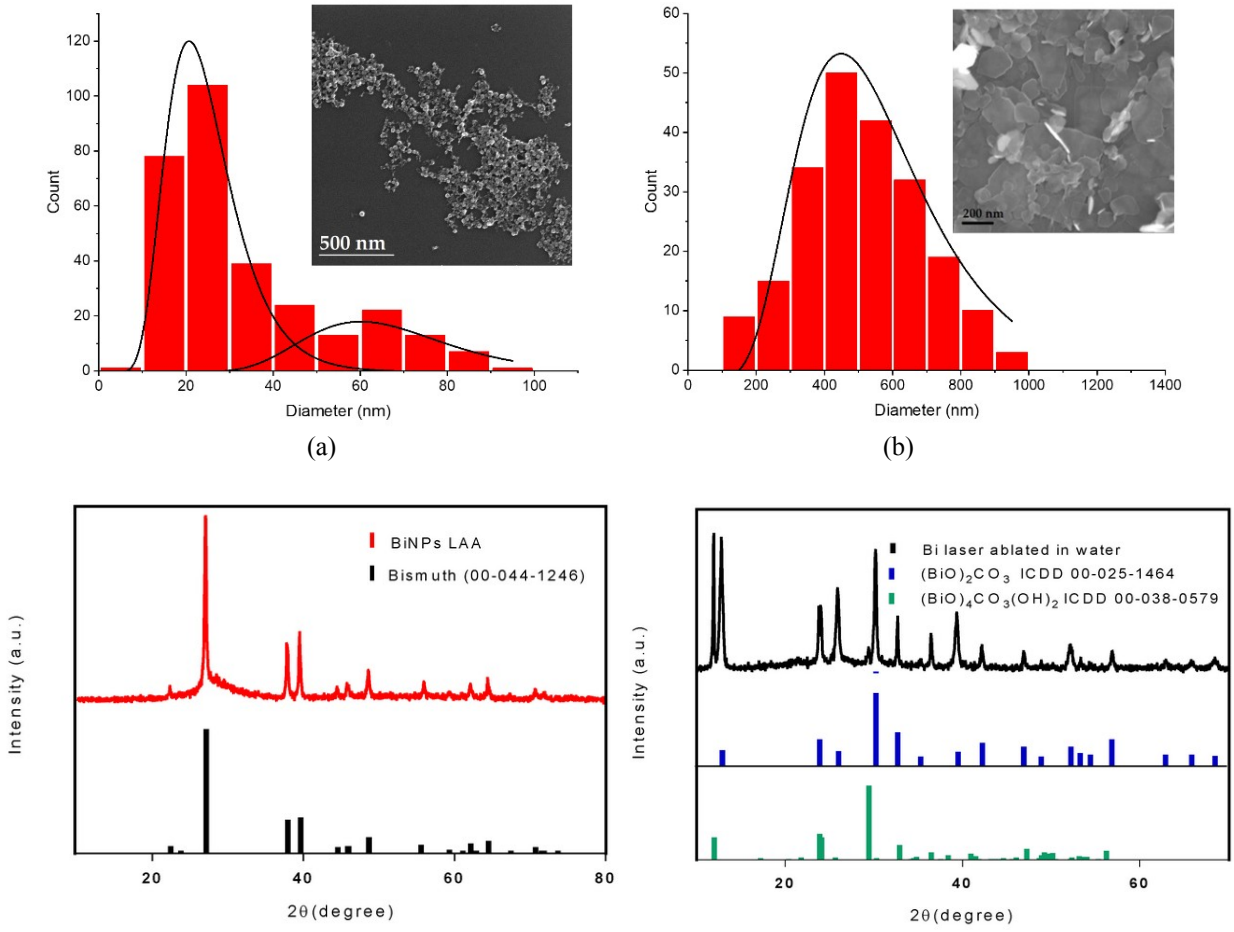

Figure 6. Size distributions and SEM & TEM images of (a) Bi NPs produced from fs LAA and (b) Bi nanosheets after fs LAW. X-ray diffraction (XRD) patterns of (c) Bi NPs produced from fs LAA and (d) Bi nanosheets after fs LAW. Adapted from [36].

According to our ζ—potential measurements, the surface potential of Bi NPs prepared by fs LAA was −20 meV, which coincides with the stability threshold for colloidal solutions and is consistent with the observed stability of our sample over time.

It was found that mean size and size dispersion of Bi NPs during the fragmentation process have the clear tendency to decrease with increase in the laser irradiation time. To determine the dependence of the Bi NPs size characteristics on the duration of the fragmentation process, the hydrodynamic size of NPs was recorded during the fragmentation process. The results of DLS hydrodynamic size measurements are shown in Figure 7b. White light supercontinuum fragmentation in liquids is an easy and fast technique, which makes possible to obtain stable colloidal solutions of Bi NPs with precise size control from 150 to 20 nm. The typical SEM image and size distribution of Bi NPs obtained by fs laser fragmentation at 100 µJ pulse energy for 1 hour are shown in Figure 7a.

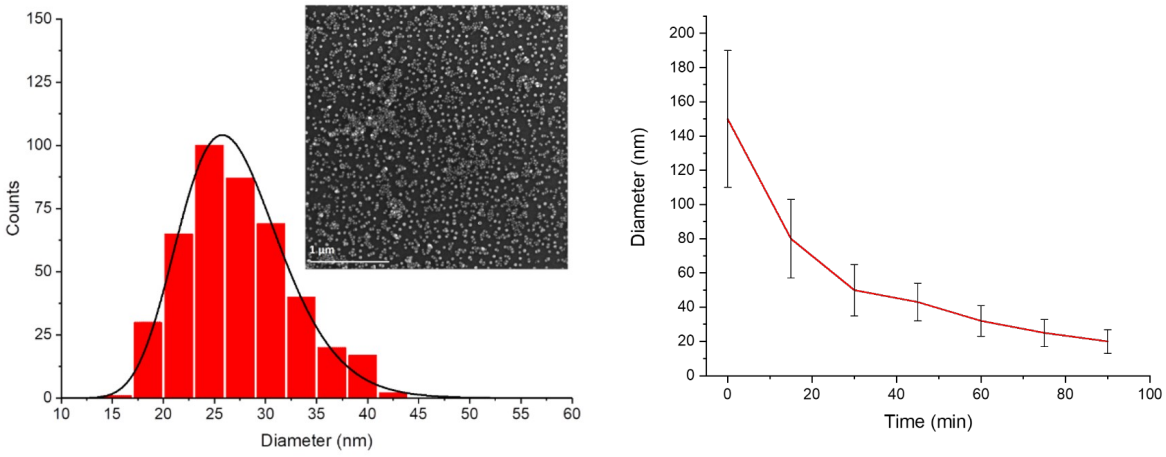

(a) (b)

Figure 7. (a) Size distribution with typical SEM image of Bi NPs obtained by fs laser fragmentation at 100 µJ pulse energy for 1 hour. (b) Dependence of Hydrodynamic diameter of Bi NPs obtained by LAA on duration of fs-laser fragmentation. Adapted from [36].

Bi NPs ablated in acetone were successfully transferred to water using a surface coating by Pluronic® F68 or F127 (Sigma-Aldrich, St. Louis, MO, USA). To achieve this surface coating, the polymer F68 or F127 was added to colloidal solution of Bi NPs in 4:1 ratio by mass and then vortexed until polymer dissolution. After this step the solution was centrifuged 10 min at 10000 RCF and the supernatant was discarded to remove the rest of the polymer. The formed pellets were resuspended in 1 mL of deionized water or PBS to produce a stable dispersion. Functionalized NPs were stored at RT for further use.

The temperature distribution dynamics induced by the nanomaterials under 808 nm laser irradiation was monitored by a thermal imaging camera FLIR A600 (FLIR Systems, Wilsonville, OR, USA). For thermal gradient dynamics measurements, all samples were prepared at a concentration of 100 µg/mL and transferred into capillary tubes (ø 300 µm, 10 mm) to avoid significant thermal convection of solvent during excitation. Each sample was then imaged in real time upon 808 nm laser irradiation of the laser beam focused in a ~15 × 50 µm waist inside the tube. Saved sequences of thermal images were processed by a FLIR camera software to plot the change in maximum temperature of the sample over time.

To determine the potential of bare and functionalized Bi NPs to be used for localized heating under NIR (808 nm) excitation for photothermal therapy, we studied the dynamics of thermal heating for both samples. The results of this study (Figure 8a and 8b) show that elemental Bi NPs demonstrated a significant increase in temperature after 30 s exposure to the NIR excitation. From the one hand, the initial rise in temperature of the elemental Bi NPs upon exposure is approximately 2 °C/ second for the first 5 s and then approximately 0.4 °C/second over the remaining 25 s, leading to a temperature maximum of 39 °C, for an overall increase of 16.5 °C. From the other hand, coated with Pluronic® Bi NPs demonstrated a significant increase in temperature, greater than that of the NPS in acetone. After 30 s exposure to the NIR excitation functionalized NPs heated up to 53 °C, for an overall increase of 24.4 °C. This suggests that the coated NPs transferred to water will be effective for use in photothermal therapy in vivo as well as for photoacoustic imaging.

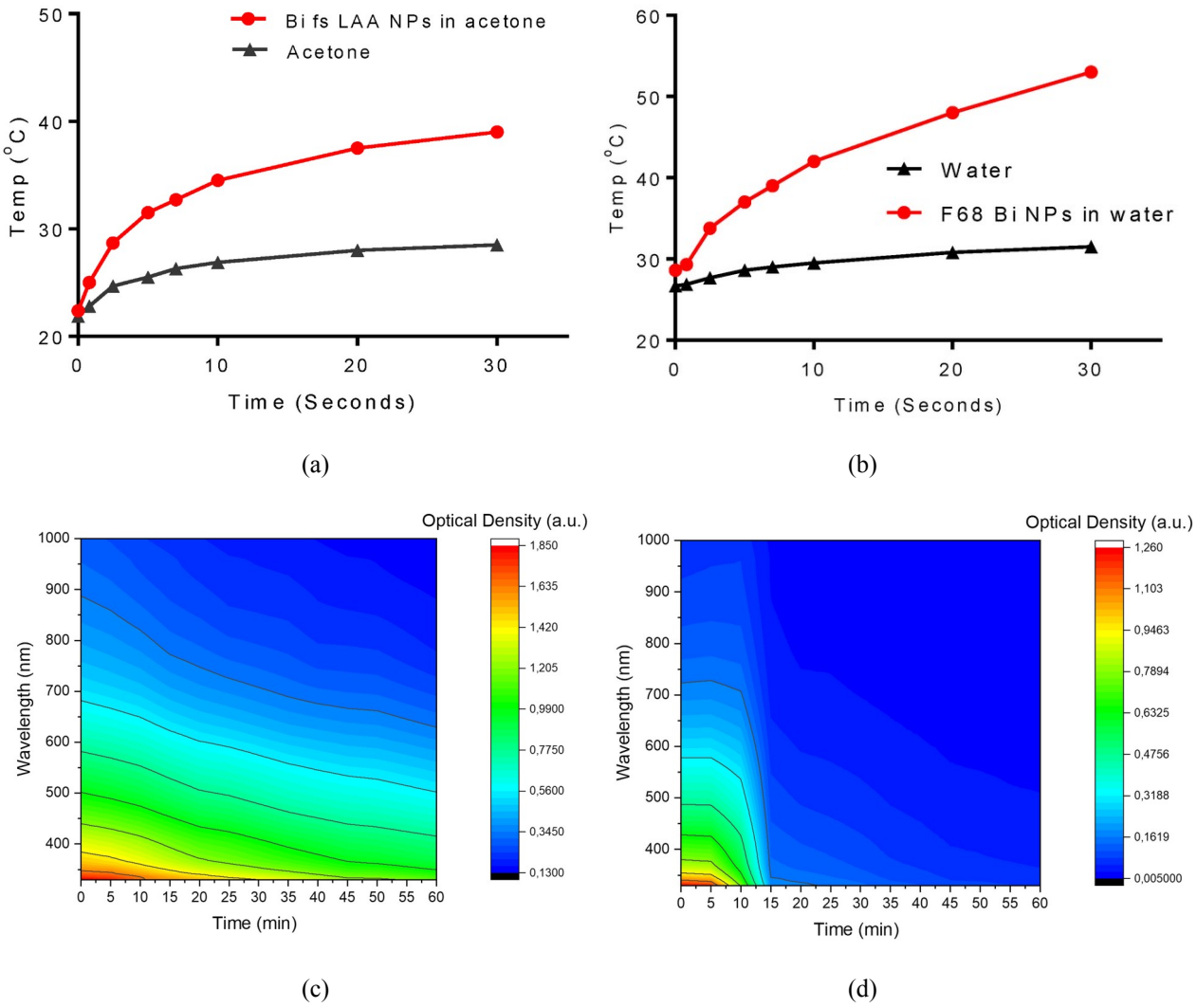

Figure 8. Photothermal heating of (a) Bi NPs produced from fs LAA and (b) Bi NPs functionalized with Pluronic® F68 in water. Dependence of extinction spectra of (c) functionalized with Pluronic® F127 Bi NPs in water and (d) initial LAA Bi NPs in PBS on time of storage obtained by the optical spectrometry method. Adapted from [36,45].

For biomedical applications, besides the fact that the NPs should be biocompatible and non-toxic, they should also be stable in biologically relevant conditions. PBS, for which osmolarity and ion concentration correspond to relative parameters in the human body, is one of the most widespread isotonic solutions used in biomedicine. The presence of a high salt content in the PBS negatively affects the colloidal stability of NPs, significantly increases their tendency to aggregation and change surface chemical composition. The protective shell in the form of a non-toxic polymer not only improve the biocompatibility and circulation time of NPs in the bloodstream, but also significantly increases their colloidal stability.

To determine the effect of surface modification of NPs on their colloidal stability in PBS and water, we detected the kinetics of changes in the optical spectra of coated and uncoated NPs. All the samples were taken at the same initial concentration. The results are shown in Figure 8c and 8d. It was found that functionalized Bi NPs have a 6.2-fold lower tendency to aggregation in PBS (time of decrease in optical density by *e* times), in contrast to bare NPs, which is a clear marker of success surface modification of NPs. The most stable were covered with Pluronic® Bi NPs in deionized water. The absence of free ions in the solution and the neutral pH of the medium has a favorable effect on the colloidal stability of NPs.

4. CONCLUSIONS

We reviewed our recent progress in laser-ablative fabrication and functionalization of some promising materials for nuclear and radiative medicine. We demonstrated that laser-ablated Si NPs functionalized with PEG can be a nearly ideal carrier of radionuclides for nuclear nanomedicine. We also described a procedure for laser synthesis of stable solutions of spherical and size-tunable (7–70 nm) ^{152}Sm-enriched samarium oxide NPs, which can be suitable for nuclear nanomedicine tasks after activation in a nuclear reactor. Finally, we demonstrated the possibility of synthesizing elemental bismuth (Bi) NPs via fs-laser ablation in water and organic solvents, promising attractive applications in radiative medicine.

5. ACKNOWLEDGEMENTS

The authors acknowledge the contribution of the Russian Science Foundation (Project 19-72-30012) for the fabrication of nanomaterials for Nuclear Nanomedicine' research. The authors acknowledge the support of Rosatom's contract 313/1655-D on 05/09/2019 for the preparation of Sm-based samples. The authors also acknowledge the contribution of the Ministry of Science and Higher Education of Russian Federation (project No 075-15-2021-1347) for the characterization of some nanomaterials. Part of this work was completed using the resources of the Chemistry Instrument Center (CIC) and supported by the office of Vice President for Research and Economic Development at the University at Buffalo, SUNY, Buffalo, NY; mail to che-ic@buffalo.edu for sample inquiries.

REFERENCES

[1] Volkert, W. A. and Hoffman, T. J., "Therapeutic Radiopharmaceuticals," Chem. Rev. 99, 2269–2292 (1999).
[2] Deyev, S. M., Waibel, R., Lebedenko, E. N., Schubiger, A. P. and Plückthun, "A. Design of multivalent complexes using the barnase-barstar module," Nature Biotech. 21, 1486–1492 (2003).
[3] Hamoudeh, M., Kamleh, M. A., Diab, R. and Fessi, H., "Radionuclides delivery systems for nuclear imaging and radiotherapy of cancer," Adv. Drug Delivery Rev. 60, 1329–1346 (2008).
[4] Mitra, A., Nan, A., Line, B. R. and Ghandehari, H., "Nanocarriers for nuclear imaging and radiotherapy of cancer," Cur. Pharm. Des. 12, 4729–4749 (2006).
[5] Matsumura, Y. and Maeda, H., "A new concept for macromolecular therapeutics in cancer chemotherapy: mechanism of tumoritropic accumulation of proteins and the antitumor agent smancs," Cancer Res. 46, 6387–6392 (1986).
[6] Mayles, P., Nahum and A., Rosenwald, J. C. [Handbook of Radiotherapy Physics: Theory and Practice], Taylor and Francis, (2007).
[7] Luderer, M. J., de la Puente, P. and Azab, A. K., "Advancements in Tumor Targeting Strategies for Boron Neutron Capture Therapy," Pharm. Res. 32, 2824–2836 (2015).
[8] Farr, J. B., Flanz, J. B., Gerbershagen, A. and Moyers, M. F., "New horizons in particle therapy systems," Med. Phys. 45, 953-983 (2018).
[9] Lee, N., Choi, S. H. and Hyeon, T., "Nano-Sized CT Contrast Agents,". Adv. Mater. 25, 2641–2660 (2013).
[10] Song, G., Cheng, L., Chao, Y., Yang, K. and Liu, Z., "Emerging Nanotechnology and Advanced Materials for Cancer Radiation Therapy," Adv. Mater. 29, 32 (2017).
[11] Kabashin, A.V., Delaporte, P., Grojo, D., Torres, R., Sarnet, T. and Sentis, M., "Nanofabrication with pulsed lasers," Nanoscale Res. Lett. 5, 454–463 (2010).
[12] Zhang, D., Gökce, B. and Barcikowski, S., "Laser synthesis and processing of colloids: Fundamentals and applications," Chem. Rev. 117, 3990–4103 (2017).
[13] Geohegan, D. B., Puretzky, A. A., Duscher, G. and Pennycook, S. J., "Time-resolved imaging of gas phase nanoparticle synthesis by laser ablation," Appl. Phys. Lett. 72, 2987–2989 (1998).
[14] Patrone, L., Nelson, D., Safarov, V. I., Sentis, M., Marine, W. and Giorgio, S., "Photoluminescence of Silicon Nanoclusters with Reduced Size Dispersion Produced by Laser Ablation", J. Appl. Phys. 87, 3829–3837 (2000).
[15] Kabashin, A.V. and Meunier, M., "Visible Photoluminescence from Nanostructured Si-Based Layers Produced by Air Optical Breakdown on Silicon," Appl. Phys. Lett. 82, 1619–1621 (2003).

[16] Kabashin, A.V. and Meunier, M., "Laser-induced treatment of silicon in air and formation of Si/SiOx photoluminescent nanostructured layers," Mater. Sci. Eng. B 101, 60–64 (2003).
[17] Kabashin, A. V, Meunier, M. and Leonelli, R., "Photoluminescence Characterization of Si-Based Nanostructured Films Produced by Pulsed Laser Ablation," J. Vac. Sci. Technol. B. 19, 2217–2222 (2001).
[18] Fojtik, A. and Henglein, A., "Laser Ablation of Films and Suspended Particles in Solvent-Formation of Cluster and Colloid Solutions," Ber. Bunsenges. Phys. Chem. 97, 252 (1993).
[19] Sibbald, M. S., Chumanov, G. and Cotton, T. M., "Reduction of Cytochrome c by Halide-Modified, Laser-Ablated Silver Colloids," J. Phys. Chem. 100, 4672-4678 (1996).
[20] Mafune, F., Kohno, J., Takeda, Y., Kondow, T., and Sawabe, H., "Formation of Gold Nanoparticles by Laser Ablation in Aqueous Solution of Surfactant," J. Phys. Chem. B. 105, 5114-5120 (2001).
[21] Dolgaev, S. I., Simakin, A.V., Vornov, V. V., Shafeev, G. A. and Bozon-Verduraz, F., "Nanoparticles Produced by Laser Ablation of Solids in Liquid Environment," Appl. Surf. Sci. 186, 546–551 (2002).
[22] Kabashin, V. K. and Meunier, M., "Synthesis of Colloidal Nanoparticles during Femtosecond Laser Ablation of Gold in Water," J. Appl. Phys. 94, 7941 (2003).
[23] Kabashin, A. V. and Meunier, M., "Femtosecond laser ablation in aqueous solutions: a novel method to synthesize non-toxic metal colloids with controllable size," J. Phys.: Conf. Series 59, 354-357 (2007).
[24] Besner, S., Degorce, J.-Y., Kabashin, A. V. and Meunier, M., "Influence of ambient medium on femtosecond laser processing of silicon," Appl. Surf. Sci. 247, 163-168 (2005).
[25] Kabashin, A. V. and Timoshenko, V. Y., "What Theranostic applications could ultrapure laser-synthesized Si nanoparticles have in cancer?," Nanomedicine 11, 2247−2250 (2016).
[26] Kabashin, A. V., Singh, A., Swihart, M. T., Zavestovskaya, I. N. and Prasad, P. N., "Laser-Processed Nanosilicon: A Multifunctional Nanomaterial for Energy and Healthcare," ACS Nano 13, 9841-9867 (2019).
[27] Maximova, K., Aristov, A., Sentis, M. and Kabashin, A.V., "Size-controllable synthesis of bare gold nanoparticles by femtosecond laser fragmentation in water," Nanotechnology 26, 065601 (2015).
[28] Kögler, M., Ryabchikov, Y. V., Uusitalo, S., Popov, A., Popov, A. A., Tselikov, G., Välimaa, A.-L., Al-Kattan, A., Hiltunen, J., Laitinen, R., Neubauer, P., Meglinski, I. and Kabashin, A. V., "Bare laser-synthesized Au-based nanoparticles as non-disturbing SERS probes for Bacteria Detection," J. Biophotonics, 11, e201700225 (2018).
[29] Baati, T. et al., "Ultrapure laser-synthesized Si-based nanomaterials for biomedical applications: in vivo assessment of safety and biodistribution," Sci. Rep. 6, 25400 (2016).
[30] Al-Kattan et al., "Ultrapure laser-synthesized Si nanoparticles with variable oxidation state for biomedical applications," J. Mater. Chem. B 4, 7852 (2016).
[31] Popov, A. A., Tselikov, G., Dumas, N., Berard, C., Metwally, K., Jones, N., Al-Kattan, A., Larrat, B., Braguer, D., Mensah, S. and et al., "Laser- synthesized TiN nanoparticles as promising plasmonic alternative for biomedical applications," Sci. Rep. 9, 1194 (2019).
[32] Zelepukin, I. V., Popov A. A., Shipunova, V. O., Tikhonowski, G. V., Mirkasymov, A. B., Popova-Kuznetsova, E. A., Klimentov, S. M., Kabashin, A. V., and Deyev, S. M., "Laser-synthesized TiN nanoparticles for biomedical applications: evaluation of safety, biodistribution and pharmacokinetics," Mat. Sci. Eng.: C 120 111717 (2021).
[33] Tikhonowski, G. V., Popova-Kuznetsova, E. A., Aleshchenko, Y. A. et al., "Effect of Oxygen on Colloidal Stability of Titanium Nitride Nanoparticles Synthesized by Laser Ablation in Liquids," Bull. Lebedev Phys. Inst. 48, 216–220 (2021).
[34] Petriev, V. M., Tischenko, V. K., Mikhailovskaya, A. A. et al., "Nuclear nanomedicine using Si nanoparticles as safe and effective carriers of ^{188}Re radionuclide for cancer therapy," Sci Rep 9, 2017 (2019).
[35] Popova-Kuznetsova, E., Tikhonowski, G., Popov, A. A., Duflot, V., Deyev, S., Klimentov, S., Zavestovskaya, I. N., Prasad, P. N., and Kabashin, A. V., "Laser-ablative synthesis of isotope-enriched samarium oxide nanoparticles for nuclear nanomedicine," Nanomaterials 10, 69 (2019).
[36] Bulmahn, J. C., Tikhonowski, G., Popov, A. A., Kuzmin, A., Klimentov, S. M., Kabashin, A. V. and Prasad, P. N., "Laser-ablative synthesis of stable aqueous solutions of elemental bismuth nanoparticles for multimodal theranostic applications", Nanomaterials 10, 1463 (2020).
[37] Sailor, M. J., [Porous silicon in practice. preparation characterization and applications], Wiley-VCH: Weinheim, Germany, 2012.

[38] Gongalsky, M. B., Osminkina, L. A., Pereira, A., Manankov, A. A., Fedorenko, A. A., Vasiliev, A. N., Solovyev, V. V., Kudryavtsev, A. A., Sentis, M., Kabashin, A. V. and Timoshenko, V. Yu., "Laser-Synthesized Oxide-Passivated Bright Si Quantum Dots for Bioimaging," Sci. Rep. 6, 24732 (2016).

[39] Kharin, A. Y., Lysenko, V. V., Rogov, A., Ryabchikov, Y. V., Geloen, A., Tishchenko, I., Marty, O. Sennikov, P. G., Kornev, R. A., Zavestovskaya, I. N., Kabashin, A. V. and Timoshenko, V. Y., "Bi-Modal Nonlinear Optical Contrast from Si Nanoparticles for Cancer Theranostics," Adv. Opt. Mater. 7, 1801728 (2019).

[40] Rioux, D., Laferriere, M., Douplik, A., Shah, D., Lilge, L., Kabashin, A. V. and Meunier, M. M., "Silicon Nanoparticles Produced by Femtosecond Laser Ablation in Water as Novel Contamination-Free Photosensitizers," J. Biomed. Opt. 14, 021010 (2009).

[41] Oleshchenko, V. A., Kharin, A. Y., Alykova, A. F., Karpukhina, O. V., Karpov, N. V., Popov, A. A., Bezotosnyi, V. V., Klimentov, S. M., Zavestovskaya, I. N., Kabashin, A. V. and Timoshenko, V. Y., "Localized infrared radiation-induced hyperthermia sensitized by laser-ablated silicon nanoparticles for phototherapy applications," Appl. Surf. Sci. 516, 145661 (2020).

[42] Tamarov, K. P., Osminkina, L. A., Zinovyev, S. V, Maximova, K. A., Kargina, J. V, Gongalsky, M. B., Ryabchikov, Y., Al-Kattan, A., Sviridov, A. P., Sentis, M., Kabashin, A. V. and Timoshenko, V. Yu., "Radio Frequency Radiation-Induced Hyperthermia Using Si Nanoparticle-Based Sensitizers for Mild Cancer Therapy," Sci. Rep. 4, 7034 (2014).

[43] Alberts, A. S., Smit, B. J., Louw, W. K. A., van Rensburg, A. J., van Beek, A., Kritzinger, V. and Nel, J. S., "Dose response relationship and multiple dose efficacy and toxicity of samarium-153-EDTMP in metastatic cancer to bone," Radiother. Oncol. 43, 175–179 (1997).

[44] Serafini, A. N., Houston, S. J., Resche, I., Quick, D. P., Grund, F. M., Ell, P. J., Bertrand, A., Ahmann, F. R., Orihuela, E., Reid, R. H., et al., "Palliation of pain associated with metastatic bone cancer using samarium-153 lexidronam: A double-blind placebo-controlled clinical trial," J. Clin. Oncol. 16, 1574–1581 (1998).

[45] Tikhonowski, G., Popov, A. A., Popova-Kuznetsova, E. A., Klimentov, S. M, Prasad, P. N. and Kabashin, A. V., "Laser-ablative synthesis of stable size-tunable Bi nanoparticles and their functionalization for radiotherapy applications," J. Phys.: Conf. Ser. 2058, 012010 (2021).